ChemComm

COMMUNICATION

View Article Online
View Journal | View Issue

Cite this: *Chem. Commun.*, 2014, **50**, 11922

Received 21st June 2014,
Accepted 12th August 2014

DOI: 10.1039/c4cc04722b

www.rsc.org/chemcomm

Type-II core–shell Si–CdS nanocrystals: synthesis and spectroscopic and electrical properties†

Guan Wang,‡[a] Jianwei Ji,‡[a] Chengdong Li,[b] Linwei Yu,[b] Weikuan Duan,[c] Wei Wei,[c] Xiaozeng You*[a] and Xiangxing Xu*[a]

Type-II Si–CdS core–shell colloidal nanocrystals (NCs) are synthesized with the spectroscopic and electronic properties tuned by the thickness of the CdS shell.

As an important semiconductor material, the group-IV element silicon (Si) is abundant on the earth and has been widely used in the electronic industry and photovoltaics.[1] The indirect bandgap nature of Si can be largely altered by the quantum confinement effect for small enough Si nanocrystals (NCs) called Si quantum dots (QDs), making Si QDs fluorescent.[2–8] Due to the high reactivity, especially, the oxidation of freshly prepared Si QDs exposed to an ambient environment, organic ligands have been used to passivate the surface of Si QDs.[8] Recently, we showed that the ligands can be functionally designed as being fluorescent, resulting in dual emission of colloidal Si QDs.[9] Another widely adopted strategy for surface protection and functionalization of QDs is to cap them with an inorganic shell.[10–14] Here we report for the first time the synthesis and characterization of quasi-monodispersed colloidal core–shell Si–CdS NCs with an elementary Si QD core and a group II–VI semiconductor CdS compound shell, forming a semiconductor heterostructure at the core–shell interface. Based on the relative alignment of the band structure, semiconductor heterostructures can be classified as type-I or type-II. For type-I, both the conduction and valence bands of one semiconductor are located within the energy gap of the other. The valence and conduction bands of CdS are, respectively, lower than those of Si at their junction, known as the type-II heterojunction.[15–17] Accordingly, Si–CdS NCs are type-II NCs. In this work, the spectroscopic and electrical properties of Si–CdS NCs were investigated, which were found to be different from CdS NCs of similar size and exhibited tunable features upon varying the thickness of the CdS shell. Si–CdS NCs are expected to have application potentials in opto-electronics as photodetector, environment sensing, light-emitting or photovoltaic devices.

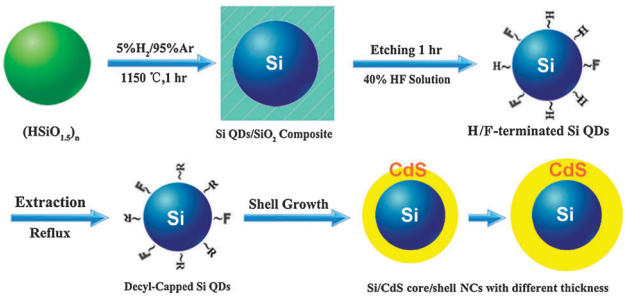

Scheme 1 Synthetic strategy of core–shell structured Si–CdS NCs.

Scheme 1 shows the synthetic strategy of Si–CdS NCs. Briefly, Si QDs were synthesized by hydrogen reduction of $(HSiO_{1.5})_n$, and etched out from the Si–SiO_2 composite by HF aqueous solution. Being extracted into the organic phase, 1-decene was modified on the surface of Si QDs to enhance the dispersibility.[8,9] The good dispersibility prevents Si QDs from aggregation during the shell growth stage. To control the CdS shell thickness and to avoid independent nucleation of CdS NCs, a modified successive ion layer adhesion and reaction (SILAR) technique[18] was applied. Face-centered cubic (fcc) structured CdS and Si have the lattice mismatch of ~6.8%, comparable to that of CdSe/CdS (~4.2%) and CdS/ZnS (~8.3%).[10,11,18] In the SILAR shell growth process, the primary addition of either a cation or an anion precursor depends on which one is more likely to get attached to the core surface.[18,19] Because it was known that the formation of Si–S bonds is the first stage for the epitaxial growth of ZnS on the Si surface,[20] the sulfur precursor was adopted as the first addition in the growth of the CdS shell on Si QDs. These Si–CdS NCs are well dispersed in nonpolar solvents such as cyclohexane or toluene.

[a] *State Key Laboratory of Coordination Chemistry, School of Chemistry and Chemical Engineering, Nanjing National Laboratory of Microstructures, Nanjing University, Nanjing 210093, P. R. China. E-mail: xuxx@nju.edu.cn, youxz@nju.edu.cn*

[b] *School of Electronics Science and Engineering, National Laboratory of Solid State Microstructures, Nanjing University, Nanjing, 210093, P. R. China*

[c] *School of Optoelectronic Engineering, Nanjing University of Posts and Telecommunications, Nanjing 210023, P. R. China*

† Electronic supplementary information (ESI) available: Experimental details of the synthesis of Si QDs, CdS and Si–CdS NCs. PL spectra, size distribution, HRTEM images, STEM images, XPS spectra and fitting parameters of the PL decay lifetime. See DOI: 10.1039/c4cc04722b

‡ G. Wang and J. W. Ji contributed equally.

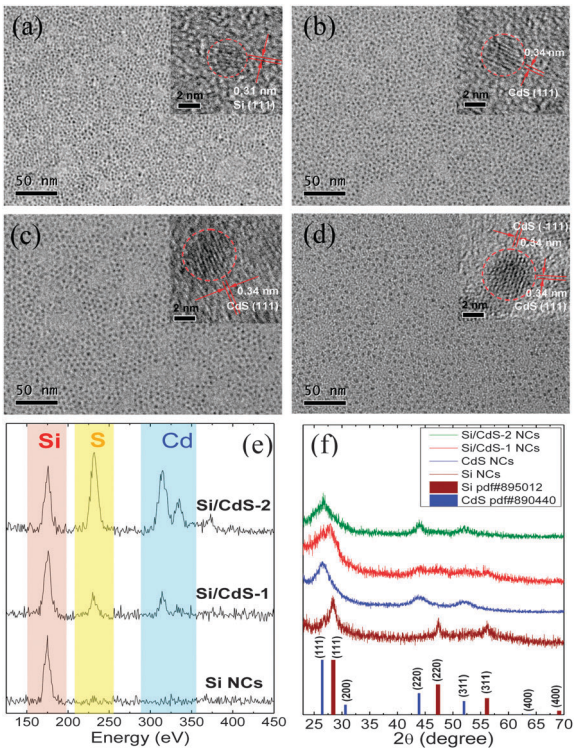

Fig. 1 TEM/HRTEM images of (a) Si QDs, (b) Si/CdS-1 NCs (c) Si/CdS-2 NCs and (d) CdS NCs. (e) EDS spectra of Si QDs, Si/CdS-1 and Si/CdS-2 NCs; and (f) the XRD pattern of the samples.

Fig. 1a–d show the typical transmission electron microscope (TEM) and the high resolution TEM (HRTEM) images of Si QDs, Si/CdS-1, Si/CdS-2 and CdS NCs, with the average diameters measured to be 2.5, 3.6, 4.5 and 4.4 nm, respectively (Fig. S2–S5, ESI†). Like CdSe/CdS NCs,[21] no clear core to shell interface can be identified by HRTEM. It may be due to the approximate lattice parameters, small size of the Si QDs and the similar image contrast of Si and CdS under HRTEM. The core–shell structure finds support from the facts that, first, the average size of NCs increases continuously with the shell growth. The size distribution of Si/CdS-2 ranges from 3.2 to 5.6 nm, separated from the size of Si QDs from 2.0 to 3.0 nm. This eliminates the possibility that Si–CdS is a mixture of Si QDs and Si–CdS NCs. Second, the {111} *d*-spacing (0.31 nm) of the Si QDs is observed by HRTEM, while for Si/CdS-2 with an average ~1.0 nm shell of CdS, the {111} *d*-spacing (0.34 nm) of CdS is observed and no *d*-spacing fringe related to Si QDs is identified, and for Si/CdS-1 with an average ~0.6 nm shell of CdS, {111} of CdS and a few {111} of Si QDs are observed. Third, the energy dispersive X-ray spectroscopy (EDS) reveals that the cadmium and sulfur to silicon ratio increases with the increase of the shell thickness (Fig. 1e). Last, Cd3d and S2p are observed by high-resolution X-ray photoelectron spectroscopy (XPS) of Si–CdS NCs (Fig. S6, ESI†), suggesting the surface capping of CdS. The XRD pattern of the Si QDs (Fig. 1f) is in good agreement with the fcc structured Si (pdf no. 895012). The broad peaks indicate the small size of the Si QDs. The sample of Si/CdS-1 shows broadened peaks composed of fcc Si and fcc CdS. While for Si/CdS-2, the XRD pattern approximates that of CdS, corresponding to the thicker shell.

Fig. 2a shows the absorption spectra. The first absorption peak appears at 385 nm for Si/CdS-1 and at 440 nm for Si/CdS-2 NCs. The red-shift should be due to the quantum confinement effect corresponding to the increase of the CdS shell thickness. The Si QDs show a long absorption tail extending to 700 nm. This feature still exists in Si/CdS-1 and Si/CdS-2, indicating the stability of Si QDs. Unlike Si QDs showing a mono-PL peak at 630 nm, the Si/CdS-1, Si/CdS-2 and CdS NCs exhibit double-peak PL spectra (Fig. 2b). The peak at the short wavelength side of CdS NCs is assigned to the band edge emission, while the relatively broad emission band at a longer wavelength side is assigned to surface states (or defect states) related emission.[22]

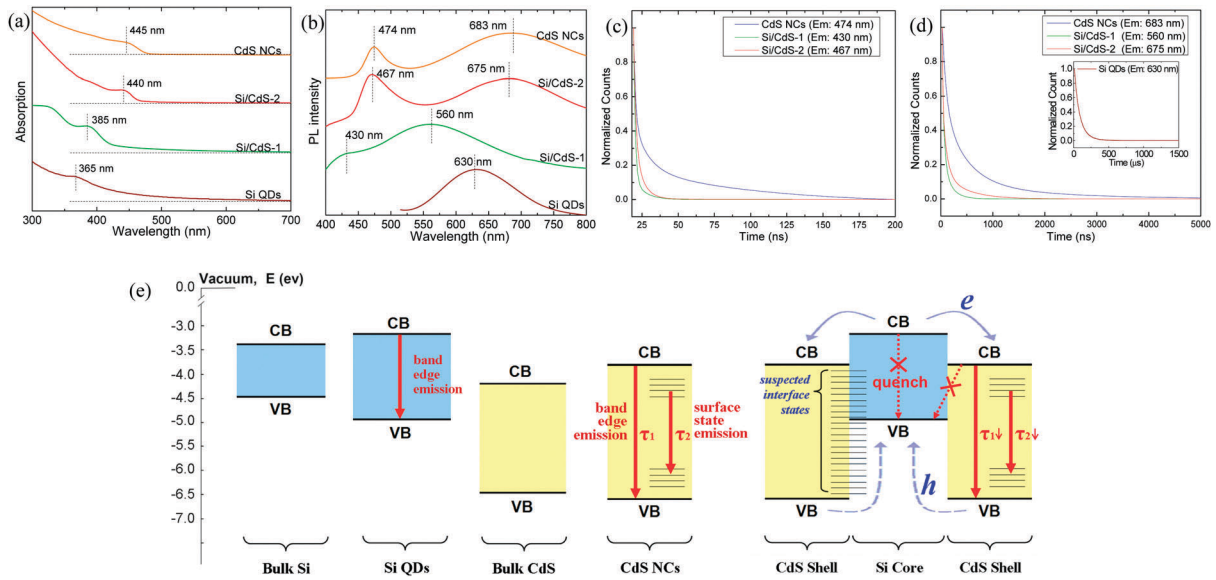

Fig. 2 Spectroscopic properties of Si QDs, CdS, Si/CdS-1 and Si/CdS-2 NCs. (a) Absorption spectra; (b) PL spectra; (c, d) PL decay curves (excitation: 360 nm). (e) Schematic illustration of the band structure diagram sketch and fluorescence of bulk Si, Si QDs, bulk CdS, CdS NCs and Si–CdS NCs.

Si/CdS-2 and CdS NCs have approximate average sizes and similar absorption and PL spectra. To verify where the PL of Si–CdS comes from and to investigate how the type-II core–shell structure affects the spectroscopic properties, decay curves of the PL were measured (Fig. 2c and d). The average PL decay lifetimes of Si/CdS-2, either for the band edge emission (9.5 ns) or for the surface state emission (288.6 ns), are much shorter than the corresponding average lifetimes of the band edge emission (70.2 ns) or the surface state emission (949.7 ns) of CdS NCs, respectively. From the bandgap alignment (Fig. 2e), we can observe that the holes tend to be confined to the Si core and the electrons reside in the CdS shell. The colloidal CdS NCs can be regarded as type-I QDs, because the bandgap of CdS NCs is within that of the insulating organic ligands.[17] Commonly, type-II QDs are expected to have longer PL decay lifetimes than the corresponding type-I QDs because of the spatial separation of charges.[17] In this investigation shorter lifetimes of the type-II Si/CdS-2 NCs were observed compared to the type-I CdS NCs, given that they have similar size and same ligands. This discrepancy suggests that the Si/CdS-2 PL spectrum should be from the CdS shell, containing no type-II emission, *i.e.* no emission from the conduction band (CB) of the CdS shell to the valence band (VB) of the Si core radiative recombination. It also suggests that the PL spectra of Si–CdS NCs do not likely contain the emission from the Si core, because the average lifetime of the Si QDs is $\sim$86 μs, which is much longer than lifetimes of CdS or Si–CdS NCs, and corresponds well with the reported typical lifetime of Si QDs.[2,23] The interface states of type-II heterojunctions of the Si core to the CdS shell may arise from defects or lattice distortion, which would induce additional non-radiative pathways for the excitation,[24] leading to shortening of the PL lifetime. The PL of Si QDs was quenched after coated with the CdS shell, which could be caused by the charge separation of the type-II structure and the charge separation time being much shorter than the PL lifetime of Si QDs. It is estimated from the band structure that if there exists the type-II PL, the spectrum should be in the range of about 900–1500 nm. However, unlike core–shell type-II NCs of CdTe–CdSe, CdSe–ZnTe or CdS–ZnSe,[17,25] type-II PL was not observed for Si–CdS NCs. We noticed that for the Si to CdS type-II heterojunction of either Si nanowires to the CdS nanowire junction at a cross point[26] or Si–CdS coaxial nanowires,[16] only luminescence from CdS was obtained and no type-II emission was reported. The absence of type-II PL of Si–CdS NCs may be due to two recombination pathways. The first is that the interface states could be a non-radiative channel; the second is the radiative and non-radiative pathways of the CdS shell, due to their decay times being shorter than the expected type-II PL lifetime. Fig. 2e combines the band structure and the suggested fluorescence mechanisms of Si, CdS and Si–CdS NCs.

The current–voltage (*I–V*) measurement (Fig. 3) revealed that the electrical resistivity of the solid CdS, Si/CdS-1 and Si/CdS-2 NCs falls within 10^3–10^4 Ω m, which is typical for CdS thin films or nanocrystals.[27] The increasing slope of the *I–V* curves with the voltage suggests that the conduction is suppressed by the Coulomb blockade at a low bias and the charge transport fall into the weak coupling regime.[28] Assuming that the CdS and Si–CdS samples have similar inter-NC distances, the lower electrical conductivity of Si–CdS NCs is probably induced by several factors. First, as an

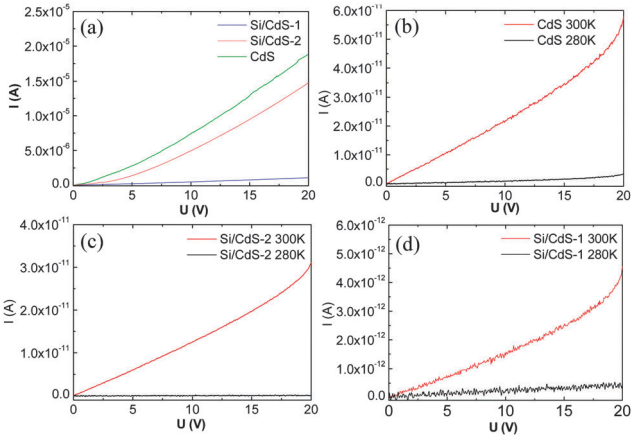

Fig. 3 Electrical conductivity of the CdS, Si/CdS-1 and Si/CdS-2 samples (a) measured under ambient air conditions, 300 K; (b)–(d) measured in vacuum at 300 K and 280 K.

n-type semiconductor, bulk CdS has much higher carrier concentration ($\sim 10^{19}$ cm^{-3}) than intrinsic Si ($\sim 10^{10}$ cm^{-3}). Therefore, the carrier concentration of Si–CdS is likely lower than that of CdS NCs of the same size. Second, the abundant interface states of the type-II heterojunction would trap the charges,[29] reducing the electrical conductivity of Si–CdS NCs. Finally, structural disorder may affect the electrical properties, because the size and structure of the NCs are distributed beyond atomic uniformity.[30] The electrical conductivity was also investigated in vacuum (<1 Pa) (Fig. 3b–d). At 280 K, all three samples exhibit a non-conductive feature. This temperature dependent conductivity is consistent with typical semiconductors. At 300 K, the conductivity decreased drastically compared with that measured in ambient air, while the relative conductivity remains CdS > Si/CdS-2 > Si/CdS-1. Trace H_2O adsorbed from air in the sample is suspected for facilitating the conductivity. A lot of attention should be paid to this for nanocrystal devices.

In conclusion, unique core–shell structured type-II Si–CdS NCs were successfully synthesized. The spectroscopic properties and electrical conductivity were tuned by the CdS shell thickness, with possible mechanisms discussed from the view-point of an energy band diagram. Hopefully, the synthesis strategy could be extended to the synthesis of a new family of colloidal core–shell nanocrystals composed of a Si QD core and the shell (or multishells) of other semiconductor materials.

This work was supported by the Major State Basic Research Development Program of China (No. 2013CB922102 and 2011CB808704), the National Natural Science Foundation of China (No. 91022031 and 21301089) and Jiangsu Province Science Foundation for Youths (BK20130562).

Notes and references

1 (*a*) G. B. Yuan, K. Aruda, S. Zhou, A. Levine, J. Xie and D. W. Wang, *Angew. Chem., Int. Ed.*, 2011, **50**, 2334; (*b*) C. Pacholski, M. Sartor, M. J. Sailor, F. Cunin and G. M. Miskelly, *J. Am. Chem. Soc.*, 2005, **127**, 11636; (*c*) L. W. Yu, B. O'Donnell, P. J. Alet, S. Conesa-Boj, F. Peiró, J. Arbiol and P. R. Cabarrocas, *Nanotechnology*, 2009, **20**, 225604; (*d*) L. W. Yu, S. Misra, J. Z. Wang, S. Y. Qian,

M. Foldyna, J. Xu, Y. Shi, E. Johnson and P. R. Cabarrocas, *Sci. Rep.*, 2014, **4**, 4357.
2 (*a*) J. G. C. Veinot, *Chem. Commun.*, 2006, 4160; (*b*) K. Dohnalova, A. N. Poddubny, A. A. Prokofiev, W. D. de Boer, C. P. Umesh, J. M. Paulusse, H. Zuilhof and T. Gregorkiewicz, *Light: Sci. Appl.*, 2013, **2**, e47; (*c*) X. Cheng, S. B. Lowe, P. J. Reece and J. J. Gooding, *Chem. Soc. Rev.*, 2014, **43**, 2680.
3 (*a*) J. R. Heath, *Science*, 1992, **258**, 1131; (*b*) N. A. Dhas, C. P. Raj and A. Gedanken, *Chem. Mater.*, 1998, **10**, 3278; (*c*) R. K. Baldwin, K. A. Pettigrew, E. Ratai, M. P. Augustine and S. M. Kauzlarich, *Chem. Commun.*, 2002, 1822; (*d*) R. D. Tilley, J. H. Warner, K. Yamamoto, I. Matsu and H. Fujimori, *Chem. Commun.*, 2005, 1833; (*e*) J. H. Warner, A. Hoshino, K. Yamamoto and R. D. Tilley, *Angew. Chem., Int. Ed.*, 2005, **44**, 4550; (*f*) R. K. Baldwin, J. Zou, K. A. Pettigrew, G. J. Yeagle, R. D. Britt and S. M. Kauzlarich, *Chem. Commun.*, 2006, 658; (*g*) R. D. Tilley and K. Yamamoto, *Adv. Mater.*, 2006, **18**, 2053; (*h*) S. W. Lin and D. H. Chen, *Small*, 2009, **5**, 72; (*i*) J. Wang, S. Q. Sun, F. Peng, L. X. Cao and L. F. Sun, *Chem. Commun.*, 2011, **47**, 4941.
4 (*a*) R. A. Bley and S. M. Kauzlarich, *J. Am. Chem. Soc.*, 1996, **118**, 12461; (*b*) K. A. Pettigrew, Q. Liu, P. P. Power and S. M. Kauzlarich, *Chem. Mater.*, 2003, **15**, 4005.
5 (*a*) D. Jurbergs, E. Rogojina, L. Mangolini and U. Kortshagen, *Appl. Phys. Lett.*, 2006, **88**, 2331161; (*b*) U. Kortshagen, L. Mangolini and A. Bapat, *J. Nanopart. Res.*, 2007, **9**, 39; (*c*) G. R. Lin, C. J. Lin and C. K. Lin, *J. Appl. Phys.*, 2005, **97**, 094306.
6 (*a*) S. M. Liu, S. Sato and K. Kimura, *Langmuir*, 2005, **21**, 6324; (*b*) S. M. Liu, Y. Yang, S. Sato and K. Kimura, *Chem. Mater.*, 2006, **18**, 637.
7 R. S. Carter, S. I. Harley, P. P. Power and M. P. Augustine, *Chem. Mater.*, 2005, **17**, 2932.
8 (*a*) E. J. Henderson and J. G. C. Veinot, *J. Am. Chem. Soc.*, 2009, **131**, 809; (*b*) E. J. Henderson, J. A. Kelly and J. G. C. Veinot, *Chem. Mater.*, 2009, **21**, 5426; (*c*) M. L. Mastronardi, F. Hennrich, E. J. Henderson, F. Maier-Flaig, C. Blum, J. Reichenbach, U. Lemmer, C. Kübel, D. Wang, M. M. Kappes and G. A. Ozin, *J. Am. Chem. Soc.*, 2011, **133**, 11928; (*d*) M. L. Mastronardi, F. Maier-Flaig, D. Faulkner, E. J. Henderson, C. Kübel, U. Lemmer and G. A. Ozin, *Nano Lett.*, 2012, **12**, 337; (*e*) C. M. Hessel, D. Reid, M. G. Panthani, M. R. Rasch, B. W. Goodfellow, J. Wei, H. Fujii, V. Akhavan and B. A. Korgel, *Chem. Mater.*, 2012, **24**, 393.
9 G. Wang, J. W. Ji and X. X. Xu, *J. Mater. Chem. C*, 2014, **2**, 1977.
10 J. J. Li, Y. A. Wang, W. Guo, J. C. Keay, T. D. Mishima, M. B. Johnson and X. Peng, *J. Am. Chem. Soc.*, 2003, **125**, 12567.
11 H. Mattoussi, J. M. Mauro, E. R. Goldman, G. P. Anderson, V. C. Sundar, F. V. Mikulec and M. G. Bawendi, *J. Am. Chem. Soc.*, 2000, **122**, 12142.
12 Z. Deng, O. Schulz, S. Lin, B. Ding, X. Liu, X. Wei, R. Ros, H. Yan and Y. Liu, *J. Am. Chem. Soc.*, 2010, **132**, 5592.
13 M. V. Kovalenko, R. D. Schaller, D. Jarzab, M. A. Loi and D. V. Talapin, *J. Am. Chem. Soc.*, 2012, **134**, 2457.
14 A. M. Dennis, B. D. Mangum, A. Piryatinski, Y. Park, D. C. Hannah, J. L. Casson, D. J. Williams, R. D. Schaller, H. Htoon and J. A. Hollingsworth, *Nano Lett.*, 2012, **12**, 5545.
15 S. Manna, S. Das, S. P. Mondal, R. Singha and S. K. Ray, *J. Phys. Chem. C*, 2012, **116**, 7126.
16 O. Hayden, A. B. Greytak and D. C. Bell, *Adv. Mater.*, 2005, **17**, 701.
17 S. Kim, B. Fisher, H. J. Eisler and M. Bawendi, *J. Am. Chem. Soc.*, 2003, **125**, 11466.
18 (*a*) J. J. Li, Y. A. Wang, W. Z. Guo, J. C. Keay, T. D. Mishima, M. B. Johnson and X. G. Peng, *J. Am. Chem. Soc.*, 2003, **125**, 12567; (*b*) R. G. Xie, U. Kolb, J. X. Li, T. Basché and A. Mews, *J. Am. Chem. Soc.*, 2005, **127**, 7480.
19 J. Ziegler, S. Xu, E. Kucur, F. Meister, M. Batentschuk, F. Gindele and T. Nann, *Adv. Mater.*, 2008, **20**, 4068.
20 B. Jaeckel, R. Fritsche, A. Klein and W. Jaegermann, *AIP Conference Proceedings ICPS-2004*, 2005, **722**, 153.
21 (*a*) S. Brovelli, R. D. Schaller, S. A. Crooker, F. García-Santamaría, Y. Chen, R. Viswanatha, J. A. Hollingsworth, H. Htoon and V. I. Klimov, *Nat. Commun.*, 2011, **2**, 280; (*b*) J. T. Zhang, Y. Tang, K. Lee and M. Ouyang, *Nature*, 2010, **466**, 91; (*c*) O. Chen, J. Zhao, V. P. Chauhan, J. Cui, C. Wong, D. K. Harris, H. Wei, H. S. Han, D. Fukumura, R. K. Jain and M. G. Bawendi, *Nat. Mater.*, 2013, **12**, 445.
22 (*a*) H. Du, G. Q. Xu, W. S. Chin, L. Huang and W. Ji, *Chem. Mater.*, 2002, **14**, 4473; (*b*) S. Vempati, Y. Ertas and T. Uyar, *J. Phys. Chem. C*, 2013, **117**, 21609.
23 F. Sangghaleh, B. Bruhn, T. Schmidt and J. Linnros, *Nanotechnology*, 2013, **24**, 225204.
24 L. Antwis, R. Gwilliam, A. Smith, K. Homewood and C. Jeynes, *Semicond. Sci. Technol.*, 2012, **27**, 035016.
25 S. A. Ivanov, A. Piryatinski, J. Nanda, S. Tretiak, K. R. Zavadil, W. O. Wallace, D. Werder and V. I. Klimov, *J. Am. Chem. Soc.*, 2007, **129**, 11708.
26 Y. Huang, X. F. Duan and C. M. Lieber, *Small*, 2005, **1**, 142.
27 (*a*) A. Ashour, N. El-Kadry and S. A. Mahmoud, *Thin Solid Films*, 1995, **269**, 117; (*b*) Y. C. Ju, S. Kim, T. G. Seong, S. Nahm, H. Chung, K. Hong and W. Kim, *Small*, 2012, **8**, 2849; (*c*) B. T. Raut, P. R. Godse, S. G. Pawar, M. A. Chougule, D. K. Bandgar, S. Sen and V. B. Patil, *J. Phys. Chem. Solids*, 2013, **74**, 236; (*d*) U. M. Jadhav, S. N. Patel and R. S. Patil, *Res. J. Mater. Sci.*, 2013, **1**, 21.
28 (*a*) D. V. Talapin, J. S. Lee, M. V. Kovalenko and E. V. Shevchenko, *Chem. Rev.*, 2010, **110**, 389; (*b*) R. Parthasarathy, X. M. Lin and H. M. Jaeger, *Phys. Rev. Lett.*, 2001, **87**, 186807.
29 C. Priester, Y. Foulon and G. Allan, *Phys. Rev. B: Condens. Matter Mater. Phys.*, 1994, **49**, 2919.
30 K. C. Beverly, J. L. Sample, J. F. Sampaio, F. Remacle, J. R. Heath and R. D. Levine, *Proc. Natl. Acad. Sci. U. S. A.*, 2002, **99**, 6456.